Materials Science & Engineering R 140 (2020) 100522

Contents lists available at ScienceDirect

Materials Science & Engineering R

journal homepage: www.elsevier.com/locate/mser

Materials for blood brain barrier modeling *in vitro*

Magali P. Ferro[a], Sarah C. Heilshorn[b,*], Roisin M. Owens[c,*]

[a] Department of Bioelectronics, Mines Saint-Étienne, 880 route de Mimet, F-13541, Gardanne, France
[b] Department of Materials Science and Engineering, Stanford University, Stanford, CA, 94305, USA
[c] Department of Chemical Engineering and Biotechnology, Philippa Fawcett Drive, CB30AS, Cambridge, UK

ARTICLE INFO

Keywords:
Blood brain barrier
Organ-on-chip
Biomaterial
Mechanotransduction
Shear stress
Basement membrane
Extracellular matrix

ABSTRACT

Brain homeostasis relies on the selective permeability property of the blood brain barrier (BBB). The BBB is formed by a continuous endothelium that regulates exchange between the blood stream and the brain. This physiological barrier also creates a challenge for the treatment of neurological diseases as it prevents most blood circulating drugs from entering into the brain. *In vitro* cell models aim to reproduce BBB functionality and predict the passage of active compounds through the barrier. In such systems, brain microvascular endothelial cells (BMECs) are cultured in contact with various biomaterial substrates. However, BMEC interactions with these biomaterials and their impact on BBB functions are poorly described in the literature. Here we review the most common materials used to culture BMECs and discuss their potential impact on BBB integrity *in vitro*. We investigate the biophysical properties of these biomaterials including stiffness, porosity and material degradability. We highlight a range of synthetic and natural materials and present three categories of cell culture dimensions: cell monolayers covering non-degradable materials (2D), cell monolayers covering degradable materials (2.5D) and vascularized systems developing into degradable materials (3D).

1. Introduction

Endothelial cells that line the inner surface of the vasculature are specialized according to the architecture and the need of the tissue it supplies [1]. In particular, brain microvascular endothelial cells (BMECs) that constitute brain capillaries, form a continuous endothelium that separates the cerebral tissue from the bloodstream. This endothelium, termed the blood brain barrier (BBB), maintains the stability of the brain tissue composition by regulating ion and macromolecule diffusion through the capillary wall [2]. The BBB ensures homeostasis in the central nervous system (CNS) by protecting neurons from the entrance of blood-circulating pathogenic agents into the brain. Therefore, CNS diseases such as amyotrophic lateral sclerosis, epilepsy, Alzheimer's and Parkinson's diseases are associated with BBB dysfunction [3–5]. Conversely, the BBB also rejects most of the large drugs (> 400 Da) targeting the brain [6]. This renders drug accumulation at relevant therapeutic concentrations challenging, for treatment of a variety of neurological diseases. The development of BBB tissue models is of great importance to understand how the microenvironment influences the BBB selectivity property and establish new therapeutic strategies for drug diffusion into the brain [7–9].

In order to build relevant BBB tissue models, it is necessary to understand the *in vivo* structure of brain capillaries. A complex and dynamic microenvironment surrounds brain capillaries and influences BBB integrity. BMECs closely interact with two other cell types, pericytes and astrocytes, which wrap 30 % and 98 % of the surface of the endothelium, respectively[10]. They provide mechanical support for the vascular endothelium and secrete biochemical factors required to maintain BBB integrity [11,12]. Pericytes and astrocytes both participate in the maturation and maintenance of BBB properties [13]. In some brain diseases, both astrocytes and pericytes affect BBB selective permeability [14,15]. For example, during inflammation astrocytes secrete pro-inflammatory mediators that increase BBB permeability and support leukocyte infiltration [14]. During cerebral ischemia, pericytes represent a source of matrix metalloproteinases (MMPs) that locally degrade the BBB and contribute to plasma leakage [15]. Both pericytes and astrocytes are separated from the BMECs by a vascular basement membrane (BM). The BM provides mechanical support to the BMECs and retains most of the biochemical cues secreted by the surrounding cells. The diffusion gradient of these biochemical cues oriented towards the BBB strongly influences BBB integrity [16,17]. Finally, as part of the vascular system, the BMECs perceive active mechanical stimuliin the form of shear stress exerted by the blood flow and the circumferential stretch induced by blood pressure [18]. Recent studies document the impact of circulatory pressure and blood flow on blood brain barrier function [18–20]. Importantly, brain endothelial cells react to shear

* Corresponding authors.
E-mail addresses: heilshorn@stanford.edu (S.C. Heilshorn), rmo37@cam.ac.uk (R.M. Owens).

https://doi.org/10.1016/j.mser.2019.100522
Received 19 July 2019; Received in revised form 26 November 2019; Accepted 30 November 2019
Available online 06 January 2020
0927-796X/ © 2020 Elsevier B.V. All rights reserved.

stress and circumferential stretch by remodeling their cytoskeletal filaments and producing stress fibers [18–20]. These fibers are aligned along the direction of flow and perpendicular to the direction of stretch. The development of BBB models to accurately predict the passage of drugs through the barrier relies on the integration of these biochemical and mechanical factors as parameters that participate in BBB maturation and function.

Two types of models are commonly used for drug testing: animal models and *in vitro* cell models. Animal models, compared to *in vitro* models, preserve the native matrix architecture and can further predict cellular response in a physiological context. However, when it comes to the BBB, there is a mismatch between animals and humans in terms of cellular and matrix composition. This usually renders animal models poorly predictive of the human BBB response. As a result, almost 80 % of animal-drug candidates fail in clinical trials due to high-level toxicity and/or low therapeutic efficiency. Conversely, *in vitro* cell models culture cells from a human origin in a well-defined environment to mimic tissue and organ functions. Various human brain endothelial cells have been successfully used to model aspects of the BBB, including immortalized cell lines, primary cells, and induced pluripotent stem cells (iPSC) [2,22,23]. BBB *in vitro* models rely on the culture of BMECs at the interface between two compartments, luminal and abluminal. Several cell culture configurations exist, which have been classified into three categories of models in this review: 2-dimensional (2D), 2.5D and 3D models. 2D models refer to the culture of BMEC monolayers on top of flat and stiff synthetic substrates [24]. Among them, the Transwell® model relies on the culture of BMECs on top of a suspended porous membrane. Transwells are commercially available and widely used to model the BBB for drug screening [25]. They offer easy access to both sides of the barrier and are relatively cheap and easy-to-use. However, they are poorly representative of BMEC native environment in term of substrate mechanical stiffness and cell curvature [26]. To overcome this limitation, soft cell-degradable materials, such as hydrogels, give rise to two main cell culture configurations [6]. The culture of BMEC monolayer inside a predesigned tubular structure made of hydrogels, named as 2.5D models in this review, and the embedding of cells into hydrogels to induce capillary angiogenesis, which we term 3D models in this review.

BMECs cultured within *in vitro* models are exposed to a variety of biochemical (*e.g.,* cell culture media composition and substrate protein coating) and physical (*e.g.,* substrate architecture and media flow) cues that may affect cell phenotype and impact the barrier formation. The impact of biochemical signaling cues on *in vitro* BBB formation and integrity is well-documented [27,28]. In the last decade, there have been multiple reports concerning the impact of shear stress on BBB integrity due to the introduction of mechanical stimuli from media flow applied to BMECs [29–31]. However, the impact of the matrix-induced mechanical signaling on *in vitro* BBB property has been poorly described (Fig. 1).

Here, we review materials that have been used as substrates to culture brain endothelial cells in 2D, 2.5D and 3D BBB models. We also explore how material properties, such as elasticity, structure, and degradability (by the cells during matrix remodeling), affect endothelial barrier function by developing an analytical framework to guide the use of BBB models. Ultimately, this review offers insight into the emerging organ-on-a-chip technology proposed as a promising option to fill the gap in drug screening. These new *in vitro* models include a variety of environmental factors, such as topographical guidance, mechanical stimulation, biochemical gradients and spatially defined co-culture [32]. BBB-on-a-chip models use biomimetic materials to culture BMECs indifferent configurations (*e.g.,* 2D, 2.5D, and 3D) to improve endothelial barrier development and maintenance.

2. The blood brain barrier basement membrane

The basement membrane (BM) acts as a physical support to the BMECs. It also constitutes a source of biochemical and biophysical cues that both modulate BBB functions and integrity. The present section describes the composition and the architecture of the BBB BM. The interaction between the endothelial cells and the BM is presented here at the molecular, cellular and tissue scale.

2.1. Architecture and composition

The extracellular matrix (ECM) is a fibrous network of entangled proteins, whose architecture and protein composition are specific to the tissue. The brain vascular BM, in particular, is secreted by neural cells during brain development and comprises four glycoprotein families: collagen IV, laminins, nidogens, and heparan sulfate proteoglycans (including perlecan and agrin) [69]. The formation of the BM depends on the self-assembly of two independent polymeric networks, one from laminin and the other from type IV collagen. First, laminin trimers self-assemble into a polymeric sheet-like structure, and this is then followed by the crosslinking of collagen fibers to create a second independent network. Finally, the two networks are linked together by nidogen and heparan glycoproteins as a result of their high affinity to both laminin and collagen (Fig. 2) [71]. The brain microvascular BM is divided into two entities that mainly differ according to their laminin isoform composition. The *endothelial BM,* secreted by BMECs, separates the endothelial cells from the pericytes. It is mainly composed of laminin-111 and –211 [16]. The *parenchymal BM,* secreted by astrocytes, comprises both laminin-411 and –511 and surrounds pericytes and BMECs [2]. The BM thickness varies from 20 to 200 nm, depending on whether the BM is lined with pericytes or astrocytes, and constitutes a reservoir of growth factors and differentiation factors secreted by surrounding cells [72,73].

The ECM contains pores and fibrils, whose size, density, and orientation together influence physicochemical matrix parameters (*e.g.* matrix rigidity, confinement, and topology) [69]. These parameters jointly impact how cells interact with the underlying matrix during tissue formation, maintenance, and regeneration [69]. BMsform thin, dense, sheet-like structures [74]. BMECs are anchored to the BM fibrils thanks to BMEC dystroglycan- and integrin-mediated adhesion complexes that interact with the laminin from the BM [75]. Apart from providing efficient guidance for cell migration, the BM also influences BBB properties on both a cellular and multicellular scale as described in the following section.

2.2. Substrate mechanosensing by vascular endothelial cells

Vascular endothelial cells are exposed to multiple mechanical stimuli, including oriented hemodynamic forces (*e.g.* shear force and circumferential stretch) and sub-endothelial matrix mechanics [76]. Vascular endothelial cells are able to probe multiple mechanical cues in parallel and translate them into an integrated response through the activation of signaling pathways. This response determines many cellular functions including motility, adhesion, and morphological stability [77–80]. The impact of BM mechanical stimuli on brain endothelial cells is attracting more attention with respect to the regulation of BBB functions.

Endothelial cells establish a physical linkage with the underlying matrix through protein complexes called focal adhesions (FA) [81]. These FA, mainly composed by integrins, give the ability to the ECs to probe the mechanical matrix properties [82], and are connected to the cell cytoskeleton [83]. This connection facilitates the transmission of mechanical forces in and out of the cell. As a consequence, cells exert pulling-pushing forces on the matrix, both mediated by the actin cytoskeleton through actin filament polymerization (pushing force) and actomyosin-dependent contraction (pulling force). In response to these forces, the matrix deforms with an amplitude that depends on the matrix elasticity and stiffness [84,85]. Endothelial cells (EC) respond to mechanical matrix properties by translating these mechanical cues into

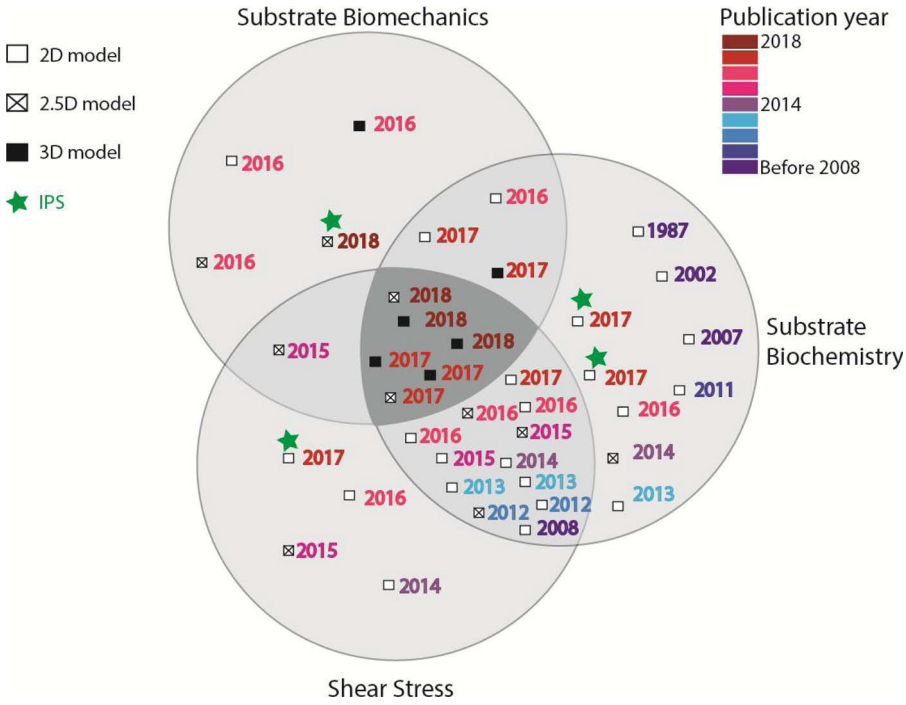

Fig. 1. Select history of *in vitro* BBB models. [11,19,29,30,33–68] A review of literature on BBB models showing year of publication and type of model, whether 2D, 2.5D or 3D. Publications were grouped for their focus on substrate biomechanics, substrate biochemistry or shear stress. IPS: induced pluripotent stem cells.

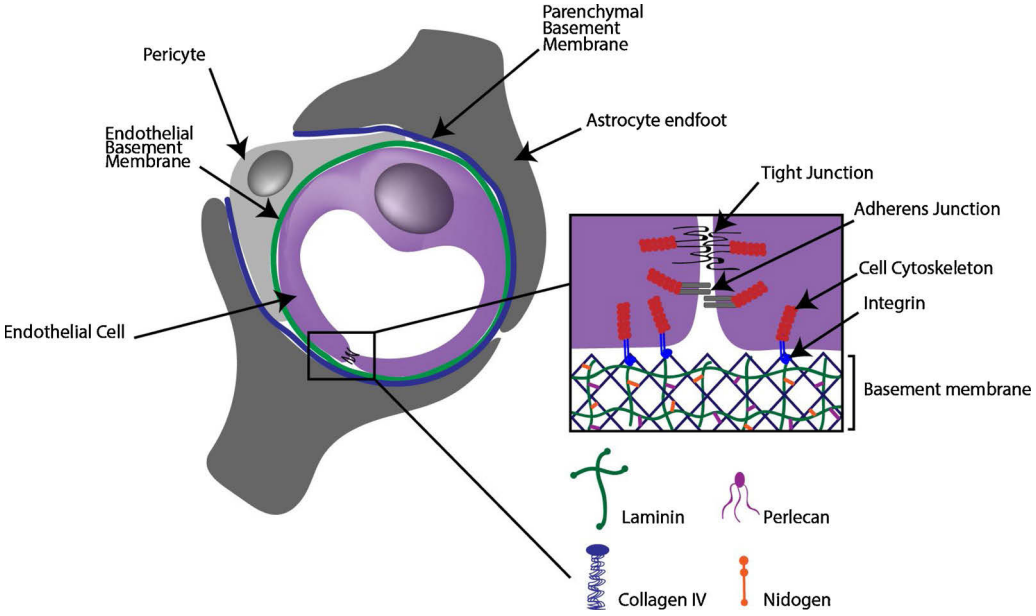

Fig. 2. Illustration of the cellular and extracellular architecture of the blood brain barrier.

biochemical signals that modulate gene and protein expression, aptly described by the term mechanotransduction [86]. In a physiological context, mechanical forces are involved in stem cell self-renewal and differentiation [87]. Tissue injury disrupts the mechanical homeostasis of the matrix that underlies normal tissue architecture. In pathological conditions, the injury results in progressive fibrosis accompanied by an increased in matrix stiffness [88]. The increase in matrix stiffness has been associated with EC barrier disruption, mainly due to a dysregulation of the G protein signaling balance [80]. Increased in tissue stiffness also plays a central role in promoting tumor-like vasculature [89].

Mechanical cues emanating from the underlying matrix also influence the overall tissue structure. [90] In the case of the BBB, in particular, the maintenance of cell-matrix interactions is critical in maintaining cell-cell adhesions and the maintenance of the all tissue architecture [91]. Indeed, these interactions stabilize numerous tight-junction (TJ) proteins, including Claudin-5, ZO-1 and Occludins, that physically close the gap between each endothelial cell and thus maintain the vascular barrier. Andresen et al. found that the vascular endothelial (VE)-cadherin, a component of the adherens junction, was related to an activated downstream mechanotransduction signal generated by substrate stiffness [72]. Indeed, endothelial cells cultured on a stiff substrate (Young's Modulus in the range of GPa) produce bundles of actin stress fibers. These stress fibers generate a tensile force in the cell that can pull proteins of the adherens junction complex away from the cell surface inward toward the center of the cells. When the number

of adherens junctions decreases, the vascular permeability increases. In contrast, the recruitment of VE-cadherin at junctional complexes has been observed within endothelial cells cultured on softer substrates (Young's Modulus in the range of kPa). In summary, the mechanical tension initiated at the FA of the EC propagates throughout the cell along the actin cytoskeleton. This tension propagates at the cell-cell adherens junctions, thereby inducing tension in the neighboring cell. The decrease in stress fiber density reduces the tensile force applied on cell-cell adherens junctions, thereby maintaining barrier tightness and function [73,92,93].

3. Materials used to culture brain vascular endothelial cells

Materials that constitute the substrate for BBB cell model tend to reproduce all or part of the BM properties. As a result of their diversity in term of physico-chemical properties, these materials may impact the formation of the BBB *in vitro* differently.

3.1. Synthetic 2D materials for the culture of brain endothelial cell monolayers

For about a century, cells have been cultured *in vitro* on flat synthetic materials. For BBB models, in particular, synthetic materials used to culture brain ECs are usually stiff (Young's Modulus in the range of MPa to GPa) and are either solid (glass or polystyrene Petri dishes) or porous (semi-permeable membranes). These surfaces provide mechanical support for cell growth, proliferation, and migration in the monolayer configuration. The substrates can be easily modified by absorptive protein surface coatings to facilitate cell adhesion and spreading. Notably, collagen IV and laminin proteins improve brain endothelial cell adhesion and proliferation and the subsequent formation of an endothelial monolayer [33,94]. Maherally et al. have shown that perlecan decreases human cerebellar microvascular endothelial cell (hCMEC/D3) barrier permeability by increasing the trans-endothelial electrical resistance (TEER), by stimulating the expression of tight junction proteins [33]. Interestingly, the influence of agrin on the BBB function seems to be dependent on cell type, improving hCMEC/D3 barrier tightness, while preventing human induced-pluripotent-stem-cell (iPSC)-derived BMEC barrier formation [34].

Porous, semi-permeable membranes are an integral component of most compartmentalized cell culture systems. Apart from providing physical support for cell growth, porous membranes help to establish cell barrier models by defining apical and basal compartments and allowing molecule exchange between them [95]. They are widely used to measure the transport of molecules across the vascular wall (*e.g.* permeability assay) in the context of drug screening [96]. Various materials have been used to fabricate porous membranes, including polycarbonate (PC), poly(ε-caprolactone) (PCL), polydimethylsiloxane (PDMS), polyester (PE), silicon nitride (SiN), and silicon dioxide (SiO_2) [95]. Polymeric track-etched membranes, such as Transwell inserts, are compatible with cell culture multiwell plates. These membranes are around 10 μm thick with a pore size ranging from 0.4–8 μm in diameter. Porous membranes with 0.4 μm diameter pores were preferentially used to culture endothelial cells since larger diameters were leading to cell migration across the membrane [95]. Nevertheless, in the case of astrocyte-endothelial cell co-cultures on opposing sides of a membrane, 3 μm pores were used to facilitate astrocyte migration through the pores toward the endothelial monolayer, thus allowing cell-cell physical contact along the endothelium [97].

Transwells membrane are made using a track-etching technique that generates randomly localized straight pores through the membrane. Because the pore distribution is not controlled, it is necessary to maintain a low pore density to prevent the formation of merges tracks and doublet holes. Several fabrication techniques based on lithography have been developed to control pore size better and distance between pores and achieve higher membrane porosity (Fig. 3). For example, Deosarkar et al. used soft lithography technique to fabricate a curved PDMS porous membrane and implement a vessel-like cell curvature [98]. Ma et al. used beam photolithography to regularly design 0.27 to 0.7 μm pores on a 1 μm-thick SiN membrane with a density of up to 50 % [100]. This ultrathin SiN membrane was shown to increase the feasibility of physical contact between astrocytes and BMECs significantly when grown on opposite sides of the membrane, thus improving BBB functions. Marino et al. used a two-photon lithography technique to design porous microtubes on top of which they cultured murine brain-derived endothelial cells (bEnd.3 cell line) [101]. Using this technique, they developed for the first time a 1 to 1 scale, biomimetic BBB model.

As part of tissue development and maintenance, cells that compose the tissue secrete and remodel their own ECM. Interestingly, this process is maintained when cells are cultured *in vitro*. Recent studies have shown that brain endothelial cells can secrete all major components of the BM when cultured on 2D synthetic materials [35]. In addition, both composition and architecture of cell-secreted ECM have been shown to influence BBB functions *in vitro* significantly [29]. In this last study, Zobel et al. cultured BMECs on an ECM secreted *in vitro* by either astrocytes, pericytes, or a serial combination of both. Analysis of the secreted ECM demonstrated that cells could remodel the underlying ECM and generate supra-structures, thus maintaining BBB functions [29]. Beyond improving cell-substrate biochemical interactions, ECM secretion by the endothelial cells might substantially influence how cells sense the mechanical properties of the underlying material. ECs cultured on top of a porous membrane were able to span ECM fibers over open pore regions. As a result, ECs established FAs over the pores. These results suggest that cells were able to locally probe ECM mechanical properties discriminating between the open pore regions and the solid substrate [105]. The number of FAs localized over the open pore region (*e.g.* sensing the secreted ECM), in comparison with the total number of FAs over the membrane, appeared to be sufficient to decrease the mechanical tension in the cells. As a result, the overall cell expression of TJs was increased, and the barrier permeability decreased. This last study has also shown that cells were only able to span fibers only over small pores (diameter < 3 μm). This observation is following previous papers showing the positive impact of 0.4 μm Transwell membrane on murine BBB functions compared to larger pores (> 3 μm) [106].

3.2. Degradable biomaterials as a matrix design element for the culture of brain vascular endothelial cell monolayers

The ECM is a dynamic structure that is continuously secreted and remodeled by cells through the action of enzymes, including matrix metalloproteinases (MMPs) [107]. The process of matrix remodeling is an essential part of tissue development and maintenance [108]. Dysregulation of this process is usually linked to tissue disease [109]. For the BBB in particular, extensive matrix remodeling of the brain vascular BM has been linked to Epilepsy and Alzheimer's disease, partly due to a change in BM mechanical properties [110–112]. In this section, we focus on cell-degradable materials that have been used to culture brain endothelial cells in monolayer for 2.5D BBB models. The physical and biochemical characteristics of these materials are summarized in Table 1.

3.2.1. Electropsun membranes

The BM is a fibrous network, whose fiber alignment and orientation influence cell and tissue functions. The electrospinning technique is a simple, versatile, and relatively inexpensive approach to generate nanofibers from a viscoelastic solution. High electric fields are applied between a metallic needle and a grounded collector to draw out a nanofiber jet from the needle tip. The nanofibers are subsequently pulled to and deposited on the collector [113]. The electrospinning parameters can be adjusted to control fiber diameter, cross-sectional shape, bead-formation, branching and fiber morphology [113,114]. Nanofibrous mats are formed by continuous electrospinning on the same area until a

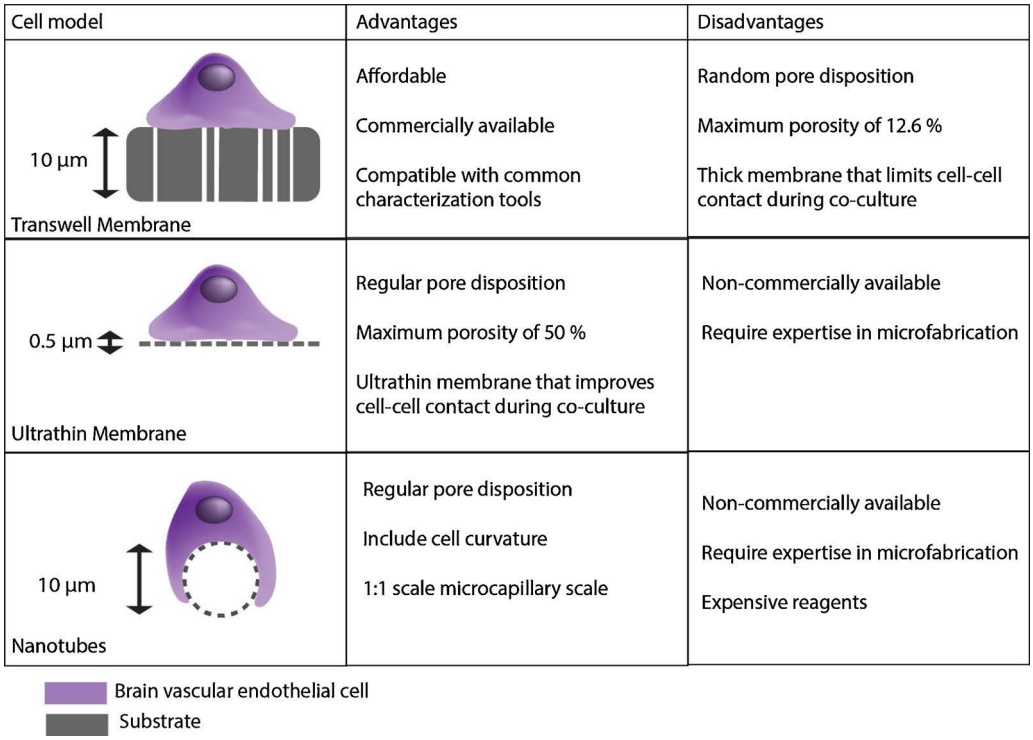

Fig. 3. Comparison of 2D blood brain barrier models. [102–104].

mat is formed. In some BBB models, nanofibrous mats replace the semi-permeable membrane from Transwell inserts [43,106]. These models remain compatible with traditional barrier tissue characterization assays and tools.

Natural polymers [116], synthetic polymers [106], and a combination of both [117] have been used to produce electrospun nanofibers. In these last studies, both material elasticity and degradation rate were tuned by varying the ratio between polymers and the crosslinking agent. Bischel et al. fabricated a 4.5 µm thick nanofibrous mat made of gelatin with a fiber diameter ranging from 100 to 600 nm [44]. Both human BMECs and astrocytes were successfully cultured for 28 days long on top of the gelatin mat. As a result, both cell matrix secretion and the expression of cell-cell TJs were upregulated when cells were cultured on top of the gelatin mat compared to the traditional Transwell porous membranes. Qi et al. used electrospun meshes made of synthetic poly(lactic-co-glycolic) acid (PLGA) to co-culture induced-pluripotent-stem (iPS)-derived ECs and astrocytes. [115] Pensabene et al. developed a 5.8 µm thick electrospun membrane made of mixed PCL and PEG polymers to culture pericytes and astrocytes with BMECs [117]. The addition of PEG increased the protein adhesion property of the fibers as well as the cell degradation rate of the membrane.

3.2.2. *Hydrogel membranes*

One significant advancement in tissue engineering has been the possibility to form hydrogels to mimic ECM mechanics and biochemistry closely [120]. Hydrogels are usually composed of a swollen polymer mesh hydrated with more than 30 % (v/w) water content. These polymers maintain their structural integrity through crosslinking between the components, where the crosslinking degree strongly influences hydrogel elasticity [121]. Hydrogels used to culture vascular endothelial cells can be composed of natural (alginate, collagen, elastin and hyaluronic acid) or synthetic (PEG, PMMA) polymers [122].

Hydrogels are compatible with a variety of fabrication techniques, including 3D printing, micropatterning, and electrospinning. These methods enable the design of different substrate configurations [121]. For example, an ultrathin hydrogel membrane was fabricated to culture Human Umbilical Vein Endothelial Cells (HUVECs) in a flat monolayer configuration [123]. In this particular study, the hydrogel was made of PEG polymer modified to include the fibronectin-derived, integrin-adhesive, tri-peptide sequence Arg-Gly-Asp (RGD). Notably, the culture of HUVECs on such membranes showed an increase in VE-cadherin expression intensity compared to the culture on a traditional porous membrane [124]. Type I collagen is one of the most favoured biomaterials used to prepare hydrogels with a low Young's Modulus (in the range of kPa) and inherent RGD sequences for cell-matrix adhesion and remodeling [31]. Hydrogel coating using fibronectin and laminin has been used to add Arg-Glu-Asp-Val (REDV) and Ile-Lys-Val-Ala-Val (IKVAV) sequences respectively. Such coatings were shown to enhance

Table 1
Materials used to replace porous membrane for 2.5D models. n.d. means 'no data'.

	Traditional porous membranes	Electrospun membranes			Hydrogel membranes	
Biomaterial/ origin	PET/ synthetic	Gelatin/ natural	PCL-PEG/ synthetic	PLGA/ synthetic	Collagen-Matrigel/ natural	PEG/synthetic
Thickness (µm)	10	4.5	5.8	30	20	9.5–18.8
Pore size (µm)	0.4	n.d.	0.6	n.d.	0.25-0.7	0.2
Fiber diameter (µm)	None	0.2	0.5	0.8	n.d.	n.d.
Stiffness	180 MPa	3.4 MPa	n.d.	53.8 MPa	660 kPa	54.7 kPa- 96.8 kPa
Physical tunability	No	Yes	Yes	Yes	Yes	Yes
References	[102]	[44]	[117]	[115]	[125]	[126]

iPS-derived BMEC barrier formation [34].

3.3. Biomaterials for blood brain barrier angiogenesis

The BBB development starts with the angiogenesis of pre-existing vessels sprouting into the embryonic neuroectoderm [27]. The communication between endothelial progenitor cells and neural cells including astrocytes and pericytes triggers brain capillary sprouting and BBB maturation [127]. The *in vitro* study of vascular network formation relies on the study of EC behavior in constricted environments, for example, embedded into a hydrogel. By culturing BMECs in monolayers, the study of these mechanisms is limited, as the cell-matrix interaction only happens on one side of the cells. This configuration forces the cells to adopt apico-basal polarity and constrains the cells' migration to only one plane [128]. In contrast, the culture of cells within a 3D matrix offers cell-matrix interactions across the entire cell surface, cell migration in any direction, and cell-cell interactions in 3D [129].

3.3.1. Angiogenesis of endothelial cells in vitro

The term "angiogenesis" refers to the development of new blood vessels. To induce angiogenic-like behavior *in vitro*, two main strategies are employed to culture endothelial cells. Cells can be suspended in a hydrogel and allowed to migrate and self-assemble to recreate a vascular network [60]. Alternatively, cells are seeded as a monolayer in contact with the hydrogel surface and expand into the gel through a sprouting mechanism [43]. More generally, endothelial cells in contact with a hydrogel and activated by angiogenic growth factors, such as the Vascular Endothelial Growth Factor (VEGF), migrate within the gel and sprout. The formation of sprouts corresponds to branch expansion from the main vessel and mainly relies on tip cells that lead the sprouting direction and stalk cells that follow tip cells and multiply to form the vessel [130]. During sprouting, endothelial cells remodel the matrix considerably through the action of MMPs able to cleave collagen fibers [131].

The tension generated mediated by cell-matrix adhesion receptors strongly influences the capillary morphogenesis [132]. Particle image velocimetry techniques were used to estimate the amplitude of cell-matrix mechanical interactions during *in vitro*EC sprouting [133]. In this last study, Du et al. described a cell-matrix interaction occurring through the tip cells' "pull" and "release" behavior during sprouting. Collagen fiber reorientation occurring during the "pulling" behavior was responsible for dynamic changes in matrix stiffness. Fibers provided 'contact guidance' along the sprout's long-axis. In a complementary study, the presence of cells within the matrix was found to be responsible for the progressive increase in matrix stiffness by both applying traction forces and depositing matrix components [134].

3.3.2. Biomaterials for blood brain barrier angiogenesis

Blood brain barrier *in vitro* angiogenesis relies on the use of hydrogels that can be remodeled by the BMECs. To the best of our knowledge, only one 3D BBB model uses PEG as a synthetic hydrogel modified to integrate the RGD peptide sequence for cell adhesion [135]. This last model includes the three major cell types for the reconstitution of a neurovascular unit: ECs, human iPSC-derived neuronal progenitors, and putative mesenchymal stem (stromal) cells. Apart from that study, most of the 3D BBB models rely on the use of natural polymer-based hydrogels, including collagen type I and fibrin.

The healing process associated with angiogenesis is usually accompanied by fibrin matrix deposition [136]. Fibrin also provides good mechanical support for angiogenesis *in vitro* [137]. Fibrin from bovine plasma was combined with various proteins from the brain vascular BM including laminin, hyaluronic acid, and chondroitin sulfate to improve BMEC interaction with the surrounding matrix [60,67]. The mechanical impact of fibrin hydrogels, influenced by matrix elasticity and fiber density, in turnstrongly influenced blood vessel formation *in vitro* [138].

Type I collagen is present in most human tissues, though its concentration in the brain parenchyma is very low. Commercially available and relatively cheap, collagen type I is widely used as a hydrogel base to culture BMECs in 3D. Collagen fibrils are self-assemble and crosslink at neutral pH to form a hydrogel [139]. Hydrogel mechanical properties are tunable by varying the collagen concentration, gelation time, temperature, pH and ionic strength [139]. Collagen concentration also influenced hydrogel fibril density and thus matrix porosity [140]. Indeed, for low collagen concentration, fibrils were sparsely distributed with a low degree of entanglement, a large mesh size, and big pores. In contrast, increased collagen concentration resulted in smaller mesh size and stiffer gels. In their study, Shamloo et al. cultured human microvascular ECs into diverse collagen concentration hydrogels. They described the collagen concentration of 2.7 mg/ml as a critical value after which cells were no longer able to elongate and penetrate the matrix [140]. McCoy et al. were able to tune collagen hydrogel microstructure by varying the gelation temperature. Indeed, decreased the gelation time of a collagen type I matrix from the usual 37 °C to 4 °C, which resulted in an increase in the length and the diameter of the fibrils [54]. The resulting changes in the hydrogel microstructure influenced the vascularization of the brain vascular endothelial cells in the matrix. Indeed, the increase in fiber length and thickness was shown to promote thick and lumenized vascular branches by more efficiently transmitting the EC contractility force along the fibers toward neighboring cells, as well as by providing strong contact guidance for vascular network development. Notably, this change in matrix microstructure was linked to an increase in collagen type IV secretion by the ECs.

4. Organ-on-a-chip systems: toward dynamic 2D, 2.5D, and 3D models

The emergence of microfabrication techniques combined with the recent progress in tissue engineering has given rise to a new class of *in vitro* models based on microfluidic devices. These new systems, named organ-on-a-chip, aim to reproduce organ functional units. This is achieved by culturing cells in a physiologically relevant microenvironment, in terms of geometrical, mechanical, and biochemical factors [141]. Microfluidic devices are particularly relevant to mimic vascular organs *in vitro*. Indeed, they propose more realistic dimensions and geometry of the vascular tissue. As a result, these devices are compatible with physiological shear stress values and physical deformation on cells [142]. Most of the BBB-on-a-chip applies physiological shear stress of 10 to 20 dyn.cm^{-2} on top of BMECs, as it was found to improve BBB function *in vitro* considerably [18,19,40].

Several materials support the fabrication of these microfluidic devices. The polydimethylsiloxane (PDMS) elastomer is widely used due to its high resolution, flexibility, optical transparency, and biocompatibility [143]. An easy way to prepare PDMS microfluidic devices is by using soft-lithography. The technique consists of pouring PDMS mixed with a crosslinker agent on top of a mold containing the design of the fluidic. After curing, the PDMS is peeled from the mold and contains its replica. The system is then closed by bonding the replica to either a glass or a PDMS flat layer, in this way creating a fluidic channel. The PDMS formulation spans a wide range of mechanical properties, including Young's Modulus varying from 500 kPa to 4 MPa [144]. However, PDMS has limitations in organ-on-chip applications due to its intrinsic hydrophobicity that may cause non-specific absorption of proteins and hydrophobic analytes, including drugs [145].

About twenty BBB-on-a-chips have been published to date, and the field is rapidly moving forward. However, the cell culture configuration varies a lot from one model to another, ranging from 2D to 3D dynamic models. Thus, for some BBB-on-a-chip systems, a porous membrane was integrated between two PDMS layers to divides the channel into two compartments [65,146]. Similar to Transwell models, cells are cultured on either side of the membrane, in which fluid composition and flow

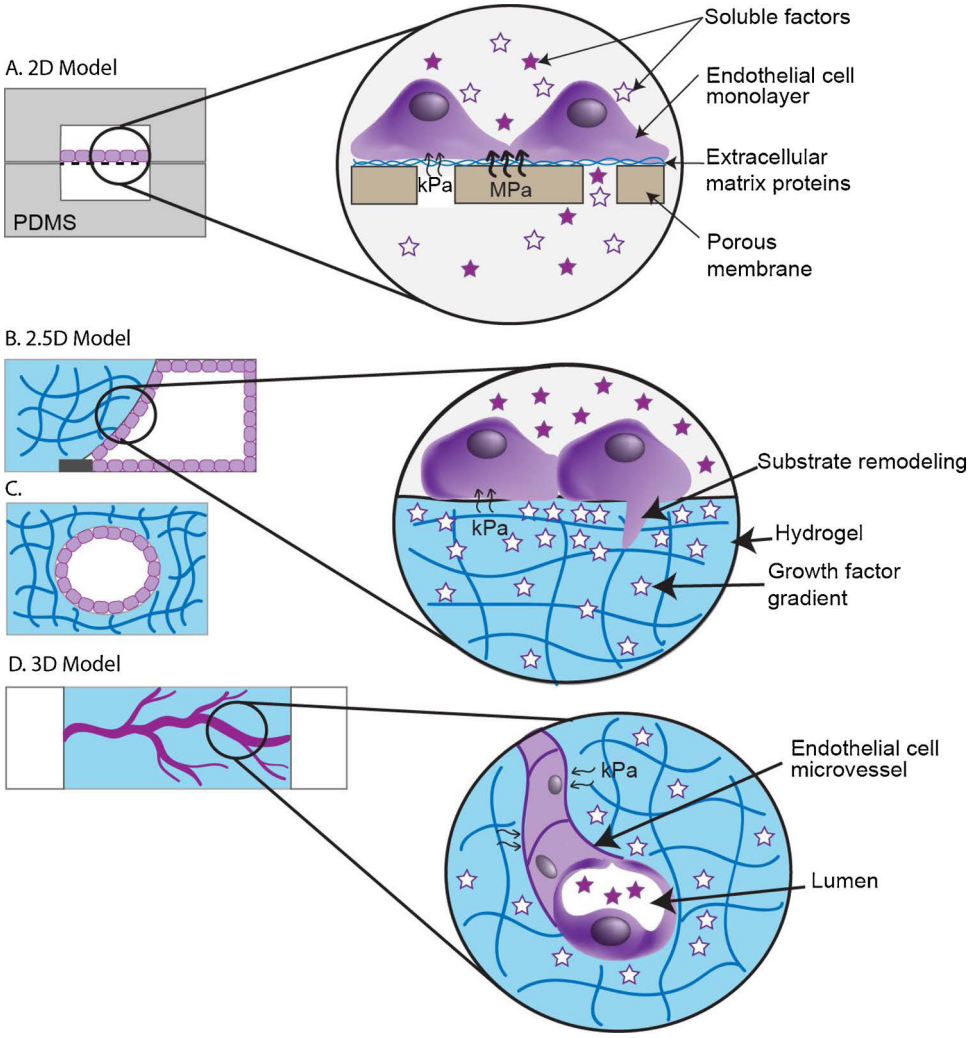

Fig. 4. Blood brain barrier-on-a-chip system, from 2D to 3D configuration.

rate are independently set (Fig. 4A) [65]. Moving toward 2.5D cell culture configurations, several organ-on-a-chip models offer the integration of hydrogels as supports for cell growth within the fluidic chamber. Lumen design for BBB-on-a-chip systems mainly relies on two techniques to separate liquids from the hydrogel. The phase guide technique is widely used for commercial organ-on-a-chip plates, such as the OrganoPlate® by the Mimetas Company, which consists of injecting the hydrogel into one channel of an interconnected multichannel device [66,147]. The presence of a phase guide in the first channel allows the gel to remain in that channel and thus create a direct interface with the adjacent channel where ECs will be cultured. In this case, the fluidic chamber for culturing cells is made of an assembly of various materials including the hydrogel and the support material for the microfluidic device (Fig. 4B). To avoid this mix of materials, an alternative strategy consists of forming a lumen directly inside the hydrogel using techniques such as viscous fingering or needle molding (Fig. 4C) [51,52]. Alternatively, the introduction of gold nanorods into a collagen hydrogel enabled the direct writing of channels by a laser beam to thermally denaturize collagen fibers with high spatial and size resolution [148]. Indeed, BMECs were encapsulated into the hydrogel and allowed to migrate into the channels and line the tubular structure to recreate a vascular network. Zheng et al. designed a 2.5D BBB model containing bifurcations, which was relevant to study the effect of local changes in shear stress on BMEC barrier integrity [64]. Finally, the tubular shape of 2.5D BBB-on-a-chip systems enabled the introduction of physiological cyclic stretch. [56,149,150] This additional mechanical parameter was found to induce EC stress fiber and FA rearrangement and influences EC barrier functions. In their 2.5D BBB model, Herland et al. also included astrocytes and pericytes directly embedded into the matrix [51]. Both pericytes and astrocytes migrated toward the vasculature to closely interact with the BMECs. As a result of these interactions, BMECs were more polarized and apt to secrete BM components such as collagen type IV.

3D BBB-on-a-chip models mainly rely on the injection of hydrogels into a central compartment delimited by two external fluidic channels. ECs are seeded in these external channels and to form adhesive contacts with the hydrogel in order to induce vascularization of the matrix (Fig. 4D) [43,66,67]. In most of the models, the mechanical interaction between BMECs and astrocytes, pericytes, or neurons, was described as essential to promote vascular angiogenesis and BBB maturation [43,60,67,151]. One hypothesis to this last observation could be that the physical support brought by the neural cells surrounding the BMECs is essential for the establishment of the BBB *in vitro*. Indeed, all previously described BBB-on-a-chips are made of hydrogels with a mechanical stiffness around 1 kPa, close to the one from the brain parenchyma [152]. Buxboim et al. suggested that cells were able to sense substrate stiffness up to 20 microns deep [153]. Considering the thickness of the BM that separates BMECs from the neural cells (nanometer range), and the cellular elastic modulus (3.5–4.2 kPa) [154] we are not able to confirm that the ECs sense the stiffness of the brain parenchyma. The use of biomaterials which enable close contact between astrocytes, pericytes, and endothelial cells is likely the best way

to reproduce the *in vivo* mechanical properties of the basement membrane.

5. Challenges and Future directions: the use of conducting polymers for *in vitro* models of electrically active NVU tissue

As illustrated in this review, biochemical and mechanical parameters strongly impact BBB integrity. The development of new, beyond-2D *in vitro* models, integrating relevant biomaterials has allowed significant progress to be made in generating more physiologically relevant models for studying the BBB. However, the inclusion of electrical cues may also be advantageous for tissue development [155]. A consensus has arisen that the BBB should not be studied in isolation, and really should be studied in the context of the neurovascular unit (NVU) [65]. As shown in Fig. 1, the NVU consists of brain capillary endothelial cells in close physical proximity to astrocytes, pericytes, and neurons. Besides the fact that the cells of the NVU share a similar environment, their function is also known to be linked. As one example, *in vivo* and *ex vivo* analysis of the impact of status epilepticus (SE) on the NVU in a rat pilocarpine model revealed an induced spatiotemporal BBB leakage happening within hours following electrical seizures. The resulting BBB damage appears to be an important factor in triggering epileptogenesis–associated changes, including degeneration of NVU cells [110]. Thus, there is an interest in understanding how brain endothelial cells react after current stimulation, in particular concerning the transport function across the BBB. Recent models using a 2D culture of b.End3 cells on a Transwell filter subjected to spatially uniform, direct current stimulation (DCS) revealed the oriented movement of fluid and solute across the BBB associated with DCS [156].

The field of neural interfacing has seen intense activity in the past decades. Although most efforts focus on *in vivo* applications involving implantation of electronic devices for recording, there has been a convergence with the field of tissue engineering, for the simple reason that modification of electrodes, to match the tissues into which they are inserted, is generally found to result in better recordings, particularly for chronic applications [157]. Extensive work has been carried out using conducting polymer (CP) hydrogels as coatings for electrodes used in neural recordings, not only because the coatings enable low impedance (and hence better recordings), but also because the CP hydrogels reduce mechanical mismatch that is the culprit for significant glial scarring incurred by implantable electrodes [158]. Another focus of work using CP hydrogels has been the idea of neural regeneration, around, or assisted by, soft electrodes [159]. Indeed, very early work focused on enhanced neurite outgrowth upon electrical stimulation of neuron-like PC12 cells grown on CP electrodes [160]. This is particularly relevant in the case of models of the NVU that involve electrically active cells.

Building on this work, biocompatible CPs incorporated into hydrogels or scaffolds are now increasingly being used in *in vitro* models, representing a new class of advanced materials combining ECM physical properties with electrical conductivity [161,162]. A variety of conducting polymers including poly(3,4-ethylenedioxythiophene) doped with poly(4-styrenesulfonate) (PEDOT:PSS) have been used for *in vitro* models of the CNS. For example, hydrogels made of PEDOT:PSS combined with polyurethane composites have been shown to support human NSC growth and enhance neurogenesis by electrical stimulation of the cells [163]. Enhanced biocompatibility of CPs by using biomolecules as dopants has led to the development of PEDOT:GAGs (glycosaminoglycans) films. These films increased the proliferation of neural cells compared to the conventional PEDOT:PSS-based substrate [164]. Neurospheres, consisting of astrocytes and neurons, grown in Matrigel and cultivated on electrodes patterned with polyethylene glycol diacrylate (PEGDA) resulted in enhanced recordings [165]. Although these materials have not been used to-date for BBB or NVU models, they show enormous potential given their interesting electrical and mechanical features. Recently, PEDOT:PSS has also been used to form mechanically compliant scaffolds [166,167] for hosting a variety of cell types [168]. These scaffolds are produced *via* a freeze-drying method, which allows easy tuning of mechanical, biological, and electrical parameters [169,170]. PEDOT:PSS PCL (polycaprolactone) composite scaffolds have been used for stimulation of electro-responsive cells showing great potential for bone reconstruction and of interest for nerve regeneration as mentioned earlier [171].

Beyond simply acting as a template for cell growth and adhesion, the electrically conducting properties of the scaffolds also allows for cell monitoring [166,172]. The use of PEDOT:PSS-based transistors, so called organic electrochemical transistors (OECTs), allows the measurement of barrier tissue integrity in real time with high temporal resolution, of particular interest for BBB permeability measurements. In addition, the proven ability of these devices to record and stimulate neurons is an added advantage when interfacing with cells of the NVU [173]. Thanks to their ability to act as a convertors of ionic signals into electrical signals, OECTs have shown promise as devices to interact with biological environments. [174] Integrated as porous 3D scaffolds or in planar configurations integrated with a microfluidic device [166,172,175,176], OECTs show a promising way to integrate continuous electrical measurement platforms into *in vitro* models, a growing trend in the organ-on-chip community (Fig. 5) [177].

In this review, we presented the physical properties of materials used to culture BMECs *in vitro* to generate models of the BBB (summarized in Table 2). Progressing from the conventional stiff and flat semi-permeable membrane, we have presented a range of materials that aim to reproduce physical cues of the brain vascular BM better. As a consequence of the rapid expansion of our understanding of mechanotransduction, and subsequent consideration of substrate physical properties such as matrix stiffness, new materials have been developed with the aim of reproducing *in vivo* mechanical cues delivered from the matrix to the tissue. Hence, new materials exhibiting a lower Young's Modulus, having increased pore density, and being capable of remodeling by surrounding cells are in high demand. The development of natural or synthetic hydrogels with tunable elasticity and cell-degradation profiles has been suggested as the most promising class of biomaterials for soft tissue engineering. Mechanical stress impact on blood brain barrier properties has been explored through organ-on-chip systems where endothelial cells are cultivated in the monolayer lining of a predesigned vascular channel [56]. We have defined the culture of a monolayer of endothelial cells on degradable substrates as a 2.5D cell culture configuration. We differentiate such models from 3D approaches consisting of embedded endothelial cells within a 3D matrix, where cells receive mechanical cues from the surrounding environment across the entire cell surface. These 3D models are particularly interesting for the study of BBB development from an angiogenesis perspective.

Declaration of Competing Interest

The authors declare that they have no known competing financial interests or personal relationships that could have appeared to influence the work reported in this paper.

Acknowledgements

R.M.O. would like to acknowledge the Ecole des Mines Saint-Etienne/Institut Mines Télécom for Bourse Ecole (M.P.F.) and the H2020 ERC CoG grant "IMBIBE" GA No. 723951ERC. M.P.F. would like to acknowledge the France-Stanford Center for Interdisciplinary Studies and the Heilshorn Biomaterials Group. S.C.H. would like to thank support from the National Science Foundation (DMR 1808415) and National Institutes of Health (R01 EB02717). M.P.F. would like to thank Nicola Cavaleri for extensive review of the manuscript.

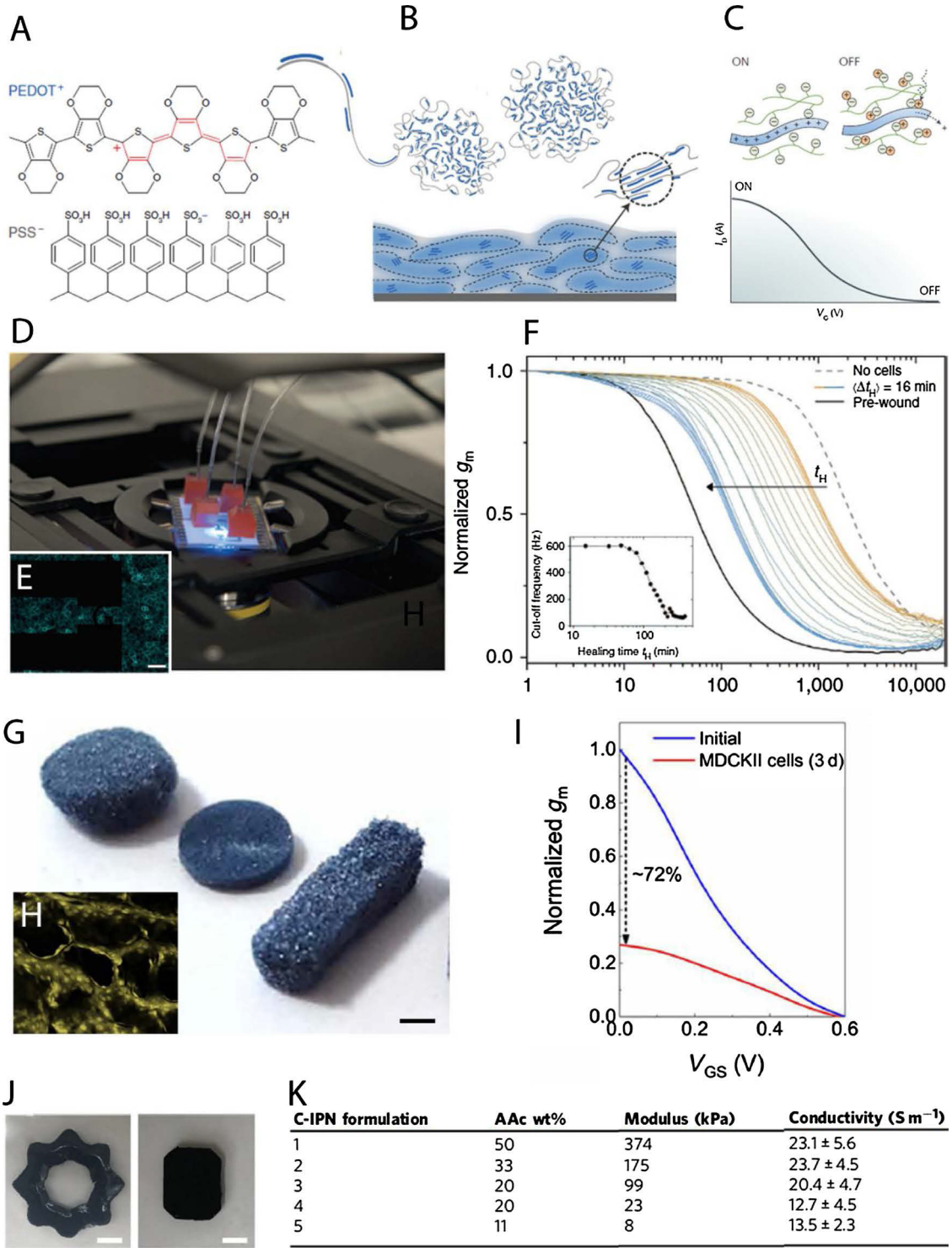

K

C-IPN formulation	AAc wt%	Modulus (kPa)	Conductivity (S m^{-1})
1	50	374	23.1 ± 5.6
2	33	175	23.7 ± 4.5
3	20	99	20.4 ± 4.7
4	20	23	12.7 ± 4.5
5	11	8	13.5 ± 2.3

Fig. 5. Conducting polymers as new material for the characterization of *in vitro* models. **A.** The chemical structure of the conducting polymer PEDOT:PSS and **B.** commonly described spatial polymer rearrangement to form a film with PEDOT:PSS rich (blue) and PSS-rich (grey) phases. [178] **C.** Transfer curve showing the operation of an organic electrochemical transistor (OECT) with a channel made of PEDOT:PSS. [179] **D.** A picture of a platform integrating planar OECTs with microfluidics and located on a microscope stage. **E.** Fluorescence image of a fully confluent layer of epithelial cells (red fluorescent protein-labelled F-actin) grown inside the microfluidic channel integrated with a planar OECT. **F.** Time evolution of the OECT frequency-dependent response during the healing process of an electrical wound generated on a confluent epithelial cell layer. [180] **G.** A picture of PEDOT:PSS scaffolds of various sizes and shapes. **H.** Fluorescence image of a PEDOT:PSS scaffold seeded with epithelial cells after 3 days of cell culture. **I.** OECT frequency-dependent response before and after cell culture. [172] **J.** A picture of PEDOT:PSS hydrogel of various size and shape. **K.** Table describing different formulation of PEDOT:PSS/acrylic acid (AAc) hydrogels and their corresponding electronic and mechanical properties [181]. (For interpretation of the references to colour in this figure legend, the reader is referred to the web version of this article).

Table 2
Summary of materials for BBB modeling and mechanical stimuli associated with investigate/improve cell-matrix interactions.

Cell model type	Mechanical stimulus	Material	Stiffness range	Endothelial cell type	Reference
2D	Curvature	SU-8 resin	GPa	bEnd.3	[101]
2D	Porosity	Silicon nitride	GPa	bBMVEC	[100]
2D	Pulsatility Shear stress	Silicon	GPa	HBMECs	[20]
2.5D	Topography	Gelatin nanofibers	MPa	HBMECs	[44]
2.5D	Topography	PCL-PEGnanofibers	n.d.	TIME cells	[117]
2.5D	Topography	PLGA nanofibers	MPa	hiPSC-derived EC	[115]
2.5D	Topography	*In vitro* cell-secreted ECM	n.d.	Porcine brain ECs	[29]
2.5D	Topography Stiffness	PEG-RGD hydrogel	kPa	HUVECs	[124]
2.5D	Topography Stiffness	Collagen-Matrigel hydrogel	kPa	HUVECs	[123]
2.5D	Geometry Shear stress	Collagen hydrogel	kPa	hBMVECs/ hCMEC/D3/ bEnd.3	[41,51,53,56]
2.5D	Shear stress Cyclic strain	Collagen-Matrigel-Hyaluronic acid hydrogel	kPa	hCMEC/D3	[56]
3D	Shear stress	Fibrin hydrogel	kPa	HUVECs/ hBMECs	[43,60,151]
3D	Topography	Collagen hydrogel	kPa	hCMECs	[54]
3D	Matrix degradability	PEG hydrogel	kPa	hPSC-derived ECs	[135]

References

[1] M. Potente, T. Mäkinen, Nat. Rev. Mol. Cell Biol. 18 (2017) 477–494.
[2] N.J. Abbott, A.A.K. Patabendige, D.E.M. Dolman, S.R. Yusof, D.J. Begley, Neurobiol. Dis. 37 (2010) 13–25.
[3] Z. Cai, P.-F. Qiao, C.-Q. Wan, M. Cai, N.-K. Zhou, Q. Li, J. Alzheimer Dis. 63 (2018) 1223–1234.
[4] J. Kealy, C. Greene, M. Campbell, Neurosci. Lett. (2018).
[5] R.G. Rempe, A.M.S. Hartz, E.L.B. Soldner, B.S. Sokola, S.R. Alluri, E.L. Abner, R.J. Kryscio, A. Pekcec, J. Schlichtiger, B. Bauer, J. Neurosci. 38 (2018) 4301–4315.
[6] M.A. Kaisar, R.K. Sajja, S. Prasad, V.V. Abhyankar, T. Liles, L. Cucullo, Expert Opin. Drug Discov. 12 (2017) 89–103.
[7] L. Di, E.H. Kerns (Eds.), Blood-Brain Barrier in Drug Discovery: Optimizing Brain Exposure of CNS Drugs and Minimizing Brain Side Effects for Peripheral Drugs, Wiley, Hoboken, New Jersey, 2015.
[8] S. Aday, R. Cecchelli, D. Hallier-Vanuxeem, M.P. Dehouck, L. Ferreira, Trends Biotechnol. 34 (2016) 382–393.
[9] L.-P. Wu, D. Ahmadvand, J. Su, A. Hall, X. Tan, Z.S. Farhangrazi, S.M. Moghimi, Nat. Commun. 10 (2019) 4635.
[10] A.D. Wong, M. Ye, A.F. Levy, J.D. Rothstein, D.E. Bergles, P.C. Searson, Front. Neuroeng. 6 (2013).
[11] S. Nakagawa, M.A. Deli, S. Nakao, M. Honda, K. Hayashi, R. Nakaoke, Y. Kataoka, M. Niwa, Cell. Mol. Neurobiol. 27 (2007) 687–694.
[12] Y. Yao, Z.-L. Chen, E.H. Norris, S. Strickland, Nat. Commun. 5 (2014) 3413.
[13] A. Armulik, G. Genové, M. Mäe, M.H. Nisancioglu, E. Wallgard, C. Niaudet, L. He, J. Norlin, P. Lindblom, K. Strittmatter, B.R. Johansson, C. Betsholtz, Nature 468 (2010) 557–561.
[14] A.T. Argaw, L. Asp, J. Zhang, K. Navrazhina, T. Pham, J.N. Mariani, S. Mahase, D.J. Dutta, J. Seto, E.G. Kramer, N. Ferrara, M.V. Sofroniew, G.R. John, J. Clin. Invest. 122 (2012) 2454–2468.
[15] R.G. Underly, M. Levy, D.A. Hartmann, R.I. Grant, A.N. Watson, A.Y. Shih, J. Neurosci. 37 (2017) 129–140.
[16] M.S. Thomsen, L.J. Routhe, T. Moos, J. Cereb. Blood Flow Metabol. 37 (2017) 3300–3317.
[17] K. Schöller, A. Trinkl, M. Klopotowski, S.C. Thal, N. Plesnila, R. Trabold, G.F. Hamann, R. Schmid-Elsaesser, S. Zausinger, Brain Res. 1142 (2007) 237–246.
[18] L. Cucullo, M. Hossain, V. Puvenna, N. Marchi, D. Janigro, BMC Neurosci. 12 (2011) 1.
[19] J.G. DeStefano, Z.S. Xu, A.J. Williams, N. Yimam, P.C. Searson, Fluids Barriers CNS 14 (2017).
[20] F. Garcia-Polite, J. Martorell, P. Del Rey-Puech, P. Melgar-Lesmes, C.C. O'Brien, J. Roquer, A. Ois, A. Principe, E.R. Edelman, M. Balcells, J. Cereb. Blood Flow Metabol. 37 (2017) 2614–2625.
[22] K. Lauschke, L. Frederiksen, V.J. Hall, Stem Cells Devel. 26 (2017) 857–874.
[23] E.S. Lippmann, A. Al-Ahmad, S.P. Palecek, E.V. Shusta, Fluids Barriers CNS 10 (2013) 1.
[24] J. Saji Joseph, S. Tebogo Malindisa, M. Ntwasa, R. Ali Mehanna (Ed.), Cell Culture, IntechOpen, 2019.
[25] R. Cecchelli, V. Berezowski, S. Lundquist, M. Culot, M. Renftel, M.-P. Dehouck, L. Fenart, Nat. Rev. Drug Discov. 6 (2007) 650–661.
[26] M. Ye, H.M. Sanchez, M. Hultz, Z. Yang, M. Bogorad, A.D. Wong, P.C. Searson, Sci. Rep. 4 (2014).
[27] B. Obermeier, R. Daneman, R.M. Ransohoff, Nat. Med. 19 (2013) 1584–1596.
[28] N.J. Abbott, A.A.K. Patabendige, D.E.M. Dolman, S.R. Yusof, D.J. Begley, Neurobiol. Dis. 37 (2010) 13–25.
[29] K. Zobel, U. Hansen, H.-J. Galla, Cell Tissue Res. 365 (2016) 233–245.
[30] D.T. Phan, R.H.F. Bender, J.W. Andrejecsk, A. Sobrino, S.J. Hachey, S.C. George, C.C. Hughes, Exper. Biol. Med. 242 (2017) 1669–1678.
[31] M.W. van der Helm, A.D. van der Meer, J.C.T. Eijkel, A. van den Berg, L.I. Segerink, Tissue Barriers 4 (2016) e1142493.
[32] B. Zhang, M. Radisic, Lab Chip 17 (2017) 2395–2420.
[33] Z. Maherally, H.L. Fillmore, S.L. Tan, S.F. Tan, S.A. Jassam, F.I. Quack, K.E. Hatherell, G.J. Pilkington, FASEB J. (2017) fj.201700162R..
[34] M.E. Katt, R.M. Linville, L.N. Mayo, Z.S. Xu, P.C. Searson, Fluids Barriers CNS 15 (2018) 7.
[35] M.S. Thomsen, S. Birkelund, A. Burkhart, A. Stensballe, T. Moos, J. Neurochem. (2016).
[36] K. Hatherell, P.-O. Couraud, I.A. Romero, B. Weksler, G.J. Pilkington, J. Neurosci. Methods 199 (2011) 223–229.
[37] Q. Xue, Y. Liu, H. Qi, Q. Ma, L. Xu, W. Chen, G. Chen, X. Xu, Int. J. Biol. Sci. 9 (2013) 174–189.
[38] A. Appelt-Menzel, A. Cubukova, K. Günther, F. Edenhofer, J. Piontek, G. Krause, T. Stüber, H. Walles, W. Neuhaus, M. Metzger, Stem Cell Rep. 8 (2017) 894–906.
[39] H. Xu, Z. Li, Y. Yu, S. Sizdahkhani, W.S. Ho, F. Yin, L. Wang, G. Zhu, M. Zhang, L. Jiang, Z. Zhuang, J. Qin, Sci. Rep. 6 (2016) 36670.
[40] Y. Takeshita, B. Obermeier, A. Cotleur, Y. Sano, T. Kanda, R.M. Ransohoff, J. Neurosci. Methods 232 (2014) 165–172.
[41] G. Adriani, D. Ma, A. Pavesi, E.L.K. Goh, R.D. Kamm, 2015 37th Annual International Conference of the IEEE Engineering in Medicine and Biology Society (EMBC), IEEE, 2015, pp. 338–341.
[42] F.E. Arthur, R.R. Shivers, P.D. Bowman, Dev. Brain Res. 36 (1987) 155–159.
[43] S. Bang, S.-R. Lee, J. Ko, K. Son, D. Tahk, J. Ahn, C. Im, N.L. Jeon, Sci. Rep. 7 (2017).
[44] L.L. Bischel, P.N. Coneski, J.G. Lundin, P.K. Wu, C.B. Giller, J. Wynne, B.R. Ringeisen, R.K. Pirlo, J. Biomed. Mater. Res. Part A 104 (2016) 901–909.
[45] R. Booth, H. Kim, Lab Chip 12 (2012) 1784.
[46] J.A. Brown, V. Pensabene, D.A. Markov, V. Allwardt, M.D. Neely, M. Shi, C.M. Britt, O.S. Hoilett, Q. Yang, B.M. Brewer, et al., Biomicrofluidics 9 (2015) 054124.
[47] H. Cho, J.H. Seo, K.H.K. Wong, Y. Terasaki, J. Park, K. Bong, K. Arai, E.H. Lo, D. Irimia, Sci. Rep. 5 (2015) 15222.
[48] C.-H. Chou, J.D. Sinden, P.-O. Couraud, M. Modo, PLoS ONE 9 (2014) e106346.
[49] L. Cucullo, N. Marchi, M. Hossain, D. Janigro, J. Cereb. Blood Flow Metabol. 31 (2011) 767–777.
[50] L.M. Griep, F. Wolbers, B. de Wagenaar, P.M. ter Braak, B.B. Weksler, I.A. Romero, P.O. Couraud, I. Vermes, A.D. van der Meer, A. van den Berg, Biomed. Microdev. 15 (2013) 145–150.
[51] A. Herland, A.D. van der Meer, E.A. FitzGerald, T.-E. Park, J.J.F. Sleeboom, D.E. Ingber, PLOS ONE 11 (2016) e0150360.
[52] J.A. Kim, H.N. Kim, S.-K. Im, S. Chung, J.Y. Kang, N. Choi, Biomicrofluidics 9 (2015) 024115.
[53] Y. Koo, B.T. Hawkins, Y. Yun, Sci. Rep. 8 (2018).
[54] M.G. McCoy, B.R. Seo, S. Choi, C. Fischbach, Acta Biomater. 44 (2016) 200–208.
[55] I. Megard, A. Garrigues, S. Orlowski, S. Jorajuria, P. Clayette, E. Ezan, A. Mabondzo, Brain Res. 927 (2002) 153–167.
[56] P.P. Partyka, G.A. Godsey, J.R. Galie, M.C. Kosciuk, N.K. Acharya, R.G. Nagele, P.A. Galie, Biomaterials 115 (2017) 30–39.
[57] B. Prabhakarpandian, M.-C. Shen, J.B. Nichols, I.R. Mills, M. Sidoryk-Wegrzynowicz, M. Aschner, K. Pant, Lab Chip 13 (2013) 1093.
[58] X. Shao, D. Gao, Y. Chen, F. Jin, G. Hu, Y. Jiang, H. Liu, Analytica Chimica Acta 934 (2016) 186–193.
[59] J.-H. Tao-Cheng, Z. Nagy, M.W. Brightman, (n.d.) 7.
[60] H. Uwamori, T. Higuchi, K. Arai, R. Sudo, Sci. Rep. 7 (2017).
[61] J.D. Wang, E.-S. Khafagy, K. Khanafer, S. Takayama, M.E.H. ElSayed, Mol. Pharm.

13 (2016) 895–906.
[62] Y.I. Wang, H.E. Abaci, M.L. Shuler, Biotechnol. Bioeng. 114 (2017) 184–194.
[63] M. Ye, H.M. Sanchez, M. Hultz, Z. Yang, M. Bogorad, A.D. Wong, P.C. Searson, Sci. Rep. 4 (2014).
[64] Y. Zheng, J. Chen, M. Craven, N.W. Choi, S. Totorica, A. Diaz-Santana, P. Kermani, B. Hempstead, C. Fischbach-Teschl, J.A. López, et al., Proc. Natl. Acad. Sci. 109 (2012) 9342–9347.
[65] B.M. Maoz, A. Herland, E.A. FitzGerald, T. Grevesse, C. Vidoudez, A.R. Pacheco, S.P. Sheehy, T.-E. Park, S. Dauth, R. Mannix, N. Budnik, K. Shores, A. Cho, J.C. Nawroth, D. Segrè, B. Budnik, D.E. Ingber, K.K. Parker, Nat. Biotechnol. (2018).
[66] N.R. Wevers, D.G. Kasi, T. Gray, K.J. Wilschut, B. Smith, R. van Vught, F. Shimizu, Y. Sano, T. Kanda, G. Marsh, S.J. Trietsch, P. Vulto, H.L. Lanz, B. Obermeier, Fluids Barrier CNS 15 (2018).
[67] S. Lee, M. Chung, N.L. Jeon, BioRxiv (2018).
[68] N.L. Stone, T.J. England, S.E. O'Sullivan, Front Cell Neurosci. 13 (2019).
[69] J. Candiello, M. Balasubramani, E.M. Schreiber, G.J. Cole, U. Mayer, W. Halfter, H. Lin, FEBS J. 274 (2007) 2897–2908.
[71] A. Pozzi, P.D. Yurchenco, R.V. Iozzo, Matrix Biol. 57–58 (2017) 1–11.
[72] R.C. Andresen Eguiluz, K.B. Kaylan, G.H. Underhill, D.E. Leckband, Biomaterials 140 (2017) 45–57.
[73] M. McRae, L.M. LaFratta, B.M. Nguyen, J.J. Paris, K.F. Hauser, D.E. Conway, Tissue Barriers (2018) e1405774.
[74] R. Jayadev, D.R. Sherwood, Curr. Biol. 27 (2017) R207–R211.
[75] K.M. Baeten, K. Akassoglou, Dev. Neurobiol. 71 (2011) 1018–1039.
[76] F.W. Charbonier, M. Zamani, N.F. Huang, Adv. Biosys. 3 (2019) 1800252.
[77] M. Gupta, B.R. Sarangi, J. Deschamps, Y. Nematbakhsh, A. Callan-Jones, F. Margadant, R.-M. Mège, C.T. Lim, R. Voituriez, B. Ladoux, Nat. Commun. 6 (2015) 7525.
[78] K. Burridge, C. Guilluy, Exp. Cell Res. 343 (2016) 14–20.
[79] S. Tojkander, G. Gateva, P. Lappalainen, J. Cell Sci. 125 (2012) 1855–1864.
[80] A.A. Birukova, X. Tian, I. Cokic, Y. Beckham, M. Gardel, K.G. Birukov, Microvasc. Res. 87 (2013) 50–57.
[81] B. Geiger, J.P. Spatz, A.D. Bershadsky, Nat. Rev. Mol. Cell Biol 10 (2009) 21–33.
[82] J.T. Parsons, A.R. Horwitz, M.A. Schwartz, Nat. Rev. Mol. Cell. Biol. 11 (2010) 633–643.
[83] S. Noria, F. Xu, S. McCue, M. Jones, A.I. Gotlieb, B.L. Langille, Am. J. Pathol. 164 (2004) 1211–1223.
[84] H.-C. Bauer, I.A. Krizbai, H. Bauer, A. Traweger, Front. Neurosci. 8 (2014).
[85] I.M. Tolić-Nørrelykke, Eur. Biophys. J. 37 (2008) 1271–1278.
[86] K.M. Gray, K.M. Stroka, Semin. Cell Dev. Biol. 71 (2017) 106–117.
[87] K.H. Vining, D.J. Mooney, Nat. Rev. Mol. Cell. Biol. 18 (2017) 728–742.
[88] D.J. Tschumperlin, G. Ligresti, M.B. Hilscher, V.H. Shah, J. Clin. Investig. 128 (2018) 74–84.
[89] F. Bordeleau, B.N. Mason, E.M. Lollis, M. Mazzola, M.R. Zanotelli, S. Somasegar, J.P. Califano, C. Montague, D.J. LaValley, J. Huynh, N. Mencia-Trinchant, Y.L. Negrón Abril, D.C. Hassane, L.J. Bonassar, J.T. Butcher, R.S. Weiss, C.A. Reinhart-King, Proceed. Natl. Acad. Sci. 114 (2017) 492–497.
[90] B. Ladoux, R.-M. Mège, Nat. Rev. Mol. Cell Biol. 18 (2017) 743–757.
[91] Y. Izawa, Y.-H. Gu, T. Osada, M. Kanazawa, B.T. Hawkins, J.A. Koziol, T. Papayannopoulou, M. Spatz, G.J. del Zoppo, J. Cereb. Blood Flow Metabol. 38 (2018) 641–658.
[92] T. Okamoto, E. Kawamoto, Y. Takagi, N. Akita, T. Hayashi, E.J. Park, K. Suzuki, M. Shimaoka, Sci. Rep. 7 (2017).
[93] P. Karki, A.A. Birukova, Pulmonary Circulation 8 (2018) 204589401877304.
[94] T. Tilling, D. Korte, D. Hoheisel, H.-J. Galla, J. Neurochem. 71 (1998) 1151–1157.
[95] H.H. Chung, M. Mireles, B.J. Kwarta, T.R. Gaborski, Lab Chip 18 (2018) 1671–1689.
[96] R. Ghaffarian, S. Muro, JoVE (2013) 50638.
[97] E. Vandenhaute, A. Drolez, E. Sevin, F. Gosselet, C. Mysiorek, M.-P. Dehouck, Lab. Investig. 96 (2016) 588–598.
[98] S.P. Deosarkar, B. Prabhakarpandian, B. Wang, J.B. Sheffield, B. Krynska, M.F. Kiani, PLoS One 10 (2015) e0142725.
[100] S.H. Ma, L.A. Lepak, R.J. Hussain, W. Shain, M.L. Shuler, Lab Chip 5 (2005) 74–85.
[101] A. Marino, O. Tricinci, M. Battaglini, C. Filippeschi, V. Mattoli, E. Sinibaldi, G. Ciofani, Small (2017) 1702959.
[102] K. Hatherell, P.-O. Couraud, I.A. Romero, B. Weksler, G.J. Pilkington, J. Neurosci. Methods 199 (2011) 223–229.
[103] A. Marino, O. Tricinci, M. Battaglini, C. Filippeschi, V. Mattoli, E. Sinibaldi, G. Ciofani, Small (2017) 1702959.
[104] S.H. Ma, L.A. Lepak, R.J. Hussain, W. Shain, M.L. Shuler, Lab Chip 5 (2005) 74–85.
[105] S.M. Casillo, A.P. Peredo, S.J. Perry, H.H. Chung, T.R. Gaborski, ACS Biomater. Sci. Eng. 3 (2017) 243–248.
[106] D.M. Wuest, A.M. Wing, K.H. Lee, J. Neurosci. Methods 212 (2013) 211–221.
[107] A. Page-McCaw, A.J. Ewald, Z. Werb, Nat. Rev. Mol. Cell Biol. 8 (2007) 221–233.
[108] J.D. Humphrey, E.R. Dufresne, M.A. Schwartz, Nat. Rev. Mol. Cell Biol. 15 (2014) 802–812.
[109] C. Bonnans, J. Chou, Z. Werb, Nat. Rev. Mol. Cell Biol. 15 (2014) 786–801.
[110] M. Bankstahl, H. Breuer, I. Leiter, M. Märkel, P. Bascuñana, D. Michalski, F.M. Bengel, W. Löscher, M. Meier, J.P. Bankstahl, W. Härtig, Eneuro 5 (2018) ENEURO.0123-18.2018.
[111] F.-X. Lepelletier, D.M.A. Mann, A.C. Robinson, E. Pinteaux, H. Boutin, Neuropathol. Appl. Neurobiol. 43 (2017) 167–182.
[112] Y. Yamazaki, T. Kanekiyo, Int. J. Mol. Sci. 18 (2017) 1965.
[113] D.H. Reneker, A.L. Yarin, Polymer 49 (2008) 2387–2425.
[114] J.I. Kim, T.I. Hwang, L.E. Aguilar, C.H. Park, C.S. Kim, Sci. Rep. 6 (2016) 23761.
[115] D. Qi, S. Wu, H. Lin, M.A. Kuss, Y. Lei, A. Krasnoslobodtsev, S. Ahmed, C. Zhang, H.J. Kim, P. Jiang, B. Duan, ACS Appl. Mater. Interfaces (2018).
[116] L.L. Bischel, P.N. Coneski, J.G. Lundin, P.K. Wu, C.B. Giller, J. Wynne, B.R. Ringeisen, R.K. Pirlo, J. Biomed. Mater. Res. Part A 104 (2016) 901–909.
[117] V. Pensabene, S.W. Crowder, D.A. Balikov, J.B. Lee, H.J. Sung, IEEE (2016) 125–128.
[120] K.Y. Lee, D.J. Mooney, Chem. Rev. 101 (2001) 1869–1880.
[121] J.-H. Lee, H.-W. Kim, J. Tissue Eng. 9 (Jan-Dec) (2018), https://doi.org/10.1177/2041731418768285 Published online 2018 Mar 29.
[122] J. Liu, H. Zheng, P. Poh, H.-G. Machens, A. Schilling, IJMS 16 (2015) 15997–16016.
[123] M.J. Mondrinos, Y.-S. Yi, N.-K. Wu, X. Ding, D. Huh, Lab Chip 17 (2017) 3146–3158.
[124] A.S. Pellowe, H.M. Lauridsen, R. Matta, A.L. Gonzalez, J. Visual. Exp. (2017).
[125] M.J. Mondrinos, Y.-S. Yi, N.-K. Wu, X. Ding, D. Huh, Lab Chip 17 (2017) 3146–3158.
[126] A.S. Pellowe, H.M. Lauridsen, R. Matta, A.L. Gonzalez, J. Visual. Exp. (2017).
[127] N.A. Malinovskaya, Y.K. Komleva, V.V. Salmin, A.V. Morgun, A.N. Shuvaev, Y.A. Panina, E.B. Boitsova, A.B. Salmina, Front. Physiol. 7 (2016).
[128] K. Duval, H. Grover, L.-H. Han, Y. Mou, A.F. Pegoraro, J. Fredberg, Z. Chen, Physiology 32 (2017) 266–277.
[129] E. Cukierman, Science 294 (2001) 1708–1712.
[130] D. Ribatti, E. Crivellato, Dev. Biol. 372 (2012) 157–165.
[131] R.G. Rempe, A.M. Hartz, B. Bauer, J. Cereb. Blood Flow Metabol. 36 (2016) 1481–1507.
[132] D.E. Ingber, Circ. Res. 91 (2002) 877–887.
[133] Y. Du, S.C.B. Herath, Q. Wang, D. Wang, H.H. Asada, P.C.Y. Chen, Sci. Rep. 6 (2016).
[134] B.A. Juliar, M.T. Keating, Y.P. Kong, E.L. Botvinick, A.J. Putnam, Biomaterials (2018).
[135] C. Barry, M.T. Schmitz, N.E. Propson, Z. Hou, J. Zhang, B.K. Nguyen, J.M. Bolin, P. Jiang, B.E. McIntosh, M.D. Probasco, S. Swanson, R. Stewart, J.A. Thomson, M.P. Schwartz, W.L. Murphy, Exp. Biol. Med. 242 (2017) 1679–1689.
[136] V.W.M. Hinsbergh, A. Collen, P. Koolwijk, Ann. N Y Acad. Sci. 936 (2006) 426–437.
[137] J. Ceccarelli, A.J. Putnam, Acta Biomaterialia 10 (2014) 1515–1523.
[138] E. Kniazeva, J.W. Weidling, R. Singh, E.L. Botvinick, M.A. Digman, E. Gratton, A.J. Putnam, Integr. Biol. 4 (2012) 431.
[139] E.E. Antoine, P.P. Vlachos, M.N. Rylander, Tissue Eng. Part B: Rev. 20 (2014) 683–696.
[140] A. Shamloo, N. Mohammadaliha, S.C. Heilshorn, A.L. Bauer, Ann. Biomed. Eng. 44 (2016) 929–941.
[141] S.N. Bhatia, D.E. Ingber, Nat. Biotechnol. 32 (2014) 760–772.
[142] K.M. Gray, K.M. Stroka, Semin. Cell Dev. Biol. 71 (2017) 106–117.
[143] B. Gale, A. Jafek, C. Lambert, B. Goenner, H. Moghimifam, U. Nze, S. Kamarapu, Inventions 3 (2018) 60.
[144] Z. Wang, A.A. Volinsky, N.D. Gallant, J. Appl. Polym. Sci. 131 (22) (2014).
[145] B.J. van Meer, H. de Vries, K.S.A. Firth, J. van Weerd, L.G.J. Tertoolen, H.B.J. Karperien, P. Jonkheijm, C. Denning, A.P. IJzerman, C.L. Mummery, Biochem. Biophys. Res. Commun. 482 (2017) 323–328.
[146] T.-E. Park, N. Mustafaoglu, A. Herland, R. Hasselkus, R. Mannix, E.A. FitzGerald, R. Prantil-Baun, A. Watters, O. Henry, M. Benz, H. Sanchez, H.J. McCrea, L.C. Goumnerova, H.W. Song, S.P. Palecek, E. Shusta, D.E. Ingber, Nat. Commun. 10 (2019) 2621.
[147] Y. Koo, B.T. Hawkins, Y. Yun, Sci. Rep. 8 (2018).
[148] K.C. Hribar, K. Meggs, J. Liu, W. Zhu, X. Qu, S. Chen, Sci. Rep. 5 (2015).
[149] R. De, Commun. Biol. 1 (2018).
[150] O.T. Guenat, F. Berthiaume, Biomicrofluidics 12 (2018) 042207.
[151] J. Kim, M. Chung, S. Kim, D.H. Jo, J.H. Kim, N.L. Jeon, PloS One 10 (2015) e0133880.
[152] S.R. Caliari, J.A. Burdick, Nat. Methods 13 (2016) 405–414.
[153] K.A. Jansen, P. Atherton, C. Ballestrem, Semin. Cell Dev. Biol. 71 (2017) 75–83.
[154] T. Yokokura, Y. Nakashima, Y. Yonemoto, Y. Hikichi, Y. Nakanishi, Int. J. Eng. Sci. 114 (2017) 41–48.
[155] C.D. McCaig, A.M. Rajnicek, B. Song, M. Zhao, Physiol. Rev. 85 (2005) 943–978.
[156] L.M. Cancel, K. Arias, M. Bikson, J.M. Tarbell, Sci. Rep. 8 (2018).
[157] D.H. Kim, M.R. Abidian, S. Richardson-Burns, S. Povlich, S.A. Spanninga, J. Hendricks, D.C. Martin, R.W. M (Ed.), Indwelling Neural Implants: Strategies for Contending with the in Vivo Environment. CRC Press (2008). CRC Press, Durham, North Carolina, 2007.
[158] R. Green, M.R. Abidian, Adv Mater 27 (2015) 7620–7637.
[159] P.M. George, A.W. Lyckman, D.A. LaVan, A. Hegde, Y. Leung, R. Avasare, C. Testa, P.M. Alexander, R. Langer, M. Sur, Biomaterials 26 (2005) 3511–3519.
[160] C.E. Schmidt, V.R. Shastri, J.P. Vacanti, R. Langer, Proc. Natl. Acad. Sci. U. S. Am. 94 (1997) 8948–8953.
[161] N.K. Guimard, N. Gomez, C.E. Schmidt, Prog. Polym. Sci. 32 (2007) 876–921.
[162] R. Balint, N.J. Cassidy, S.H. Cartmell, Acta Biomaterialia 10 (2014) 2341–2353.
[163] M. Javadi, Q. Gu, S. Naficy, S. Farajikhah, J.M. Crook, G.G. Wallace, S. Beirne, S.E. Moulton, Macromol. Biosci. 18 (2018) 1700270.
[164] D. Mantione, I. del Agua, W. Schaafsma, J. Diez-Garcia, B. Castro, H. Sardon, D. Mecerreyes, Macromol. Biosci. 16 (2016) 1227–1238.
[165] J. Pas, C. Pitsalidis, D.A. Koutsouras, P.P. Quilichini, F. Santoro, B. Cui, L. Gallais, R.P. O'Connor, G.G. Malliaras, R.M. Owens, Adv. Biosys. 2 (2018) 1700164.
[166] S. Inal, A. Hama, M. Ferro, C. Pitsalidis, J. Oziat, D. Iandolo, A.-M. Pappa, M. Hadida, M. Huerta, D. Marchat, P. Mailley, R.M. Owens, Adv. Biosyst. 1 (2017)

1700052.
[167] A.G. Guex, J.L. Puetzer, A. Armgarth, E. Littmann, E. Stavrinidou, E.P. Giannelis, G.G. Malliaras, M.M. Stevens, Acta Biomater. 62 (2017) 91–101.
[168] D. Iandolo, F.A. Pennacchio, V. Mollo, D. Rossi, D. Dannhauser, B. Cui, R.M. Owens, F. Santoro, Adv. Biosyst. 3 (2019) 1800103.
[169] I. del Agua, S. Marina, C. Pitsalidis, D. Mantione, M. Ferro, D. Iandolo, A. Sanchez-Sanchez, G.G. Malliaras, R.M. Owens, D. Mecerreyes, ACS Omega 3 (2018) 7424–7431.
[170] A.K. Jayaram, C. Pitsalidis, E. Tan, C.-M. Moysidou, M.F.L. De Volder, J.-S. Kim, R.M. Owens, Front. Chem. 7 (2019).
[171] D. Iandolo, A. Ravichandran, X. Liu, F. Wen, J.K.Y. Chan, M. Berggren, S.-H. Teoh, D.T. Simon, Adv. Healthc. Mater. 5 (2016) 1505–1512.
[172] C. Pitsalidis, M.P. Ferro, D. Iandolo, L. Tzounis, S. Inal, R.M. Owens, Sci. Adv. 4 (2018) eaat4253.
[173] D. Khodagholy, T. Doublet, P. Quilichini, M. Gurfinkel, P. Leleux, A. Ghestem, E. Ismailova, T. Herve, S. Sanaur, C. Bernard, G.G. Malliaras, Nat. Commun. 4 (2013) 1575.
[174] J. Rivnay, M. Ramuz, P. Leleux, A. Hama, M. Huerta, R.M. Owens, Appl. Phys. Lett. 106 (2015) 043301.
[175] V.F. Curto, B. Marchiori, A. Hama, A.-M. Pappa, M.P. Ferro, M. Braendlein, J. Rivnay, M. Fiocchi, G.G. Malliaras, M. Ramuz, R.M. Owens, Microsyst. Nanoeng. 3 (2017) 17028.
[176] V.F. Curto, M.P. Ferro, F. Mariani, E. Scavetta, R.M. Owens, Lab Chip 18 (2018) 933–943.
[177] M.W. van der Helm, O.Y.F. Henry, A. Bein, T. Hamkins-Indik, M.J. Cronce, W.D. Leineweber, M. Odijk, A.D. van der Meer, J.C.T. Eijkel, D.E. Ingber, A. van den Berg, L.I. Segerink, Lab Chip 19 (2019) 452–463.
[178] J. Rivnay, S. Inal, B.A. Collins, M. Sessolo, E. Stavrinidou, X. Strakosas, C. Tassone, D.M. Delongchamp, G.G. Malliaras, Nat. Commun. 7 (2016) 11287.
[179] J. Rivnay, S. Inal, A. Salleo, R.M. Owens, M. Berggren, G.G. Malliaras, Nat. Rev. Mater. 3 (2018) 17086.
[180] V.F. Curto, B. Marchiori, A. Hama, A.-M. Pappa, M.P. Ferro, M. Braendlein, J. Rivnay, M. Fiocchi, G.G. Malliaras, M. Ramuz, R.M. Owens, Microsyst. Nanoeng. 3 (2017) 17028.
[181] V.R. Feig, H. Tran, M. Lee, Z. Bao, Nat. Commun. 9 (2018).

Dr. Magali Ferro is currently a research associate at the University of Cambridge working on the NEPLEX Project (kidney on chip)under the guidance of Dr. Shery Huang. Following a degree in biotechnology at ENSAT in Toulouse and AgroParisTech, she did a Masters at the Unversity of Pierre and Marie Curie in Paris, specialising in neuroscience. She carried out her PhD in the dept. of bioelectronics at Ecole des Mines de St. Etienne, on the microelectronics campus in Provence under the supervision of Róisín M. Owens, working on *in vitro* models of human tissues, in particular the neurovascular unit.

Professor Sarah Heilshorn completed her undergraduate studies in chemical engineering at Georgia Tech. She then earned her MS and PhD in chemical engineering at the California Institute of Technology (Caltech) under the supervision of David A. Tirrell. While a graduate student, she was also a visiting scholar in the Department of Polymer Science at the Kyoto Institute of Technology through a National Science Foundation East Asia Fellowship. She was awarded the Caltech Everhart Lectureship for her PhD thesis work in 2004. Following this, Prof. Heilshorn was a postdoctoral scholar with Mu-ming Poo at the University of California, Berkeley in the Department of Molecular and Cell Biology. In 2006 she joined Stanford University as an Assistant Professor in the Department of Materials Science & Engineering. She also holds courtesy faculty appointments in the Departments of Bioengineering and Chemical Engineering. Her research laboratory studies the dynamics of biological and bio-inspired systems at multiple length scales, including the molecular through to the multi-cellular level. Current topics of investigation include the design of injectable materials for stem cell and drug delivery, protein-engineered materials for regenerative medicine scaffolds, and peptide-based self-assembly materials for templated nanoparticle synthesis. In 2009, she was selected for the National Science Foundation CAREER Award and the National Institutes of Health New Innovator Award for young faculty. She has received many additional awards including the 3M Non-Tenured Faculty Award in 2014 and the University of Sydney International Research Collaboration Award in 2015. She has been elected fellow of the Royal Society of Chemistry and the American Institute for Medical and Biological Engineering.

Dr. Róisín M. Owens is a University Lecturer at the Dept. of Chemical Engineering and Biotechnology in the University of Cambridge and a Fellow of Newnham College. She received her BA in Natural Sciences (Mod. Biochemistry) at Trinity College Dublin, and her PhD in Biochemistry and Molecular Biology at Southampton University. She carried out two postdoc fellowships at Cornell University, on host-pathogen interactions of *Mycobacterium tuberculosis* in the dept. of Microbiology and Immunology with Prof. David Russell, and on rhinovirus therapeutics in the dept. of Biomedical Engineering with Prof. Moonsoo Jin. From 2009–2017 she was a group leader in the dept. of bioelectronics at Ecole des Mines de St. Etienne, on the microelectronics campus in Provence. Her current research centers on application of organic electronic materials for monitoring biological systems *in vitro*, with a specific interest in studying the gut-brain-microbiome axis. She has received several awards including the European Research Council starting (2011), proof of concept grant (2014) and consolidator (2016) grants, a Marie Curie fellowship, and an EMBO fellowship. In 2014, she became principle editor for biomaterials for MRS communications (Cambridge University Press), and she serves on the advisory board of Advanced BioSystems and Journal of Applied Polymer Science (Wiley). She is author of 70+ publications and 2 patents. She is a 2019 laureate of the Suffrage Science award.